

1 **Brief communication: Intercomparison study reveals pathways for**  
2 **improving the representation of sea-ice biogeochemistry in models**

3 Letizia Tedesco<sup>1</sup>, Giulia Castellani<sup>2,3</sup>, Pedro Duarte<sup>4</sup>, Meibing Jin<sup>5</sup>, Sebastien Moreau<sup>4</sup>, Eric Mortenson<sup>6</sup>,  
4 Benjamin Tobey Saenz<sup>7</sup>, Nadja Steiner<sup>8,9,10</sup>, Martin Vancoppenolle<sup>11</sup>

5 <sup>1</sup>Marine and Freshwater Solutions, Finnish Environment Institute, Helsinki, Finland

6 <sup>2</sup>Institute of Environmental Physics (IUP), University of Bremen, Bremen, Germany

7 <sup>3</sup>Deutsches Zentrum für Luft- und Raumfahrt (DLR), Institut für Physik der Atmosphäre, Oberpfaffenhofen, Germany

8 <sup>4</sup>Norwegian Polar Institute, Tromsø, Norway

9 <sup>5</sup>University of Alaska Fairbanks, AK, USA

10 <sup>6</sup>University of Miami, Cooperative Institute for Marine and Atmospheric Studies (CIMAS)

11 <sup>7</sup>Biota.Earth, Berkeley, CA, USA

12 <sup>8</sup>Institute of Ocean Sciences, Fisheries and Oceans Canada, Sidney, BC, Canada

13 <sup>9</sup>Canadian Center for Climate Modelling and Analysis, Environment and Climate Change Canada, Victoria, BC, Canada

14 <sup>10</sup>School of Earth and Ocean Sciences, University of Victoria, Victoria, BC, Canada

15 <sup>11</sup>Laboratoire d'Océanographie et du Climat, CNRS/IRD/MNHN, Sorbonne Université, Paris, France

16

17 *Correspondence to:* Letizia Tedesco (letizia.tedesco@environment.fi)

18

19 **Abstract.** Sea-ice biogeochemical models are key to understanding polar marine ecosystems. We present an intercomparison  
20 of six one-dimensional models, assessing their ability to simulate algal phenology and nutrient dynamics using physical-  
21 biogeochemical data from an Arctic drift expedition in spring 2015. While no model fully captured observed bloom dynamics  
22 with default settings, tuning improved biomass but had a limited impact on nutrients. The experiment revealed challenges in  
23 simulating short-lived, dynamic ice habitats, which are expected to become more common in a changing Arctic. Variability in  
24 tuning strategies underscores key knowledge gaps and highlights the need for coordinated future model developments to  
25 improve reliability and predictive capacity.

26 **1 Introduction**

27 Sea ice is home to an active microbial community, with ice algae displaying some of the highest Chlorophyll-a (Chl-a)  
28 concentrations of any aquatic environment (Arrigo, 2017). Ice algae play multiple pivotal roles in polar oceans, representing  
29 the largest biomass fraction in sea ice (Poulin et al., 2011), contributing to overall marine primary production (Dalman et al,  
30 2025), acting as a critical food source for the marine food web, especially during winter (Schaafsma et al., 2017), and efficiently  
31 contributing to the ocean carbon sink (Boetius et al., 2013). Together with phytoplankton, ice algae form the foundation of the  
32 polar marine food web, supporting key under-ice foraging species such as Arctic cod (*Boreogadus saida*) in the Arctic Ocean  
33 (Geoffroy et al., 2023) and Antarctic krill (*Euphausia superba*) in the Southern Ocean (Kohlbach et al., 2017). These species

34 depend on the presence of sea ice and play a crucial role in transferring carbon to higher trophic levels, including humans  
35 (Steiner et al., 2021).

36  
37 Current environmental changes are placing considerable pressure at the base of the food web, triggering significant effects  
38 throughout trophic levels (e.g., Post et al., 2013; Koch et al., 2023). Despite the recognised importance of the sea-ice  
39 ecosystems (Lannuzel et al., 2020), our knowledge remains limited due to their remote location and extreme weather  
40 conditions, which restrict observational data - particularly biological observations - to sparse spatial and temporal distributions.  
41 As a result, the representation of sea-ice biological and ecological processes in numerical models has historically been limited.  
42 However, in recent decades, significant advances have been made in modelling sea-ice habitats and the evolution of sea-ice  
43 biological communities (Castellani et al., 2025). Progress includes improved representation of physical processes, greater  
44 biodiversity, and enhanced ecosystem complexity.

45  
46 An intercomparison of three-dimensional models has already been conducted to understand similarities and differences in  
47 simulated ice algae abundance and distribution, the Ice Algae Model Intercomparison Project – Phase 1 (IAMIP1, Watanabe  
48 et al., 2019). This study investigated the seasonal-to-decadal variability in ice-algal primary productivity across four Arctic  
49 regions during 1980–2009, as simulated by five participating models. Its conclusions indicated that, despite the ongoing  
50 reduction in Arctic sea ice, the decadal trend in ice-algal productivity remained unclear. The vernal bloom shifted towards an  
51 earlier onset and shorter duration over the simulated period, and the choice of maximum algal growth rate was identified as a  
52 key driver of inter-model differences in simulated ice-algal primary productivity. A second phase, expanding the study’s scope  
53 to global coverage and centennial timescales following CMIP6 (Coupled Model Intercomparison Project Phase 6, Eyring et  
54 al., 2016) protocols, is currently underway (IAMIP2, Hayashida et al., 2021). However, given the numerous limitations and  
55 uncertainties associated with these large-scale models, they are more useful for deriving bulk properties than for investigating  
56 more detailed ecological processes.

57  
58 To this end, one-dimensional (1D) process models become essential for addressing knowledge gaps in sea-ice biogeochemistry  
59 and ecological dynamics, as they provide a level of detail that large-scale models lack. They also allow for direct comparisons  
60 with in-situ observations, improving the ability to validate results. However, existing process models have been developed  
61 independently during periods of limited observations and incomplete process understanding, validated by observations at  
62 different locations, leading to substantial differences across models. These differences make an intercomparison of models  
63 performances challenging. To address this, the BEPSII (Biogeochemical Exchange Processes at Sea-Ice Interfaces,  
64 <https://www.bepsii.org>) expert group initiated an intercomparison of 1D sea-ice biogeochemical models, presented here,  
65 aiming at: i) understanding variability among models in representing key processes and responses to a common set of boundary  
66 conditions, ii) identifying divergences in models’ behaviour, the variety of tuning strategy, and the drivers of model sensitivity,  
67 iii) testing transferability, and finally iv) promoting harmonisation for future model developments. The focus has been on

68 understanding the similarities and differences in simulated ice algae dynamics and investigating the controlling factors  
69 responsible for the temporal variability and magnitude of ice-algal productivity among participating 1D models.

70  
71 We present in this study an intercomparison of 1D sea-ice biogeochemical models (briefly described in Sect. 2.1 and more  
72 comprehensively in Appendix A), focusing on their ability to simulate ice algal dynamics and nutrient cycling. Using a refrozen  
73 lead time series (described in Sect 2.2) as a test case, we assess model performance through a structured comparison of  
74 simulated and observed biogeochemical variables. Two experiments - *no tuning* and *tuning* - were conducted (Sect 2.3) to  
75 evaluate the baseline model configurations as well as the impact of targeted parameter adjustments on model accuracy. We  
76 analyse differences in model outputs, identify key sources of variability, and discuss the challenges associated with simulating  
77 ice algal growth and nutrient fluxes (Sect 3). Finally, we highlight the implications of our findings for future model  
78 development and propose directions for improving the representation of biogeochemical processes in sea-ice models (Sect. 4).

79 **2 Methods**

80 **2.1 Sea-ice biogeochemical models**

81 1D process models are typically designed to represent only vertical processes, assuming that horizontal advection is negligible.  
82 Since they are computationally efficient, these models can incorporate a high level of ecosystem complexity, such as  
83 representing multiple functional groups of organisms and providing high vertical resolution by discretising sea ice into several  
84 layers.

85  
86 1D sea-ice biogeochemical models vary in vertical resolution, ecosystem complexity, and whether they are coupled to the  
87 ocean and/or atmosphere (Castellani et al., 2025). The biogeochemically active part of sea ice, also known as the Biologically  
88 Active Layer (BAL) (Tedesco et al., 2010), is represented either as a single layer near the ice-ocean interface of prescribed or  
89 variable thicknesses depending on sea-ice permeability, or as multiple layers spanning the vertical range of the sea ice with an  
90 active brine network (e.g., Jeffery et al., 2016). Single-layer approaches are computationally more efficient than multi-layer  
91 models. A single-layer model of variable thicknesses in response to thermodynamic growth, often referred to as dynamic  
92 layering, provides a more realistic representation of bottom community dynamics (Tedesco et al., 2010). Multi-layer models,  
93 on the other hand, capture the vertical variability of biogeochemical variables and allow simulating surface and infiltration  
94 communities.

95  
96 As in ocean models, the structure of sea-ice microbial ecosystems is represented using a set of “Plankton Functional Types”  
97 (PFTs), which in our model framework include sea-ice algae, sea-ice heterotrophic bacteria, and sea-ice fauna such as grazers,  
98 and non-living inorganic (e.g., sea-ice micro- and macronutrients) and organic matter (e.g., sea-ice detritus). The simplest  
99 models are N-P models, which include only one nutrient (N) and one algal functional type (P). The elemental composition of

100 ice algae is typically fixed, based on prescribed Redfield carbon, nitrogen, silicon, phosphorous ratios (106:16:16:1), along  
101 with fixed Chl-a:carbon ratios. The more comprehensive N-P-Z-D models also include grazers (Z) (such as sea-ice fauna) and  
102 sea-ice detritus (D). In the simplest version of these models, only one limiting nutrient is considered. More complex models  
103 may represent multiple nutrients and different PFTs for ice algal communities, as well as bacteria and grazers. In simpler  
104 models, the processes associated with bacterial remineralisation or grazing are often implicitly parameterised using constant  
105 rates.

106  
107 The intercomparison included five modelling teams and a total of six model configurations. These models varied in several  
108 aspects, encompassing differences in physical and biogeochemical process complexity, radiation schemes, vertical resolution,  
109 choice of limiting nutrient, area of original tuning of the model, and coupling to an interactive sea-ice physical model and/or  
110 ocean biogeochemical model of various complexity. Table 1 summarises the main commonalities and differences among the  
111 models. For more details on a specific model, we refer to the model's original reference (Table 1) and further description in  
112 Appendix A.

113  
114 Most of the models had interactive physical components, while only one (i.e., SIMBA) required prescribed ice physics.  
115 Additionally, only half of the models were coupled to an interactive ocean biogeochemical model. Among the sea-ice physical  
116 models, complexities ranged from a Semtner 0-layer scheme (SM 0L) to multi-layer energy-conserving models (EC ML). All  
117 models, except one, used a single-band radiation transfer scheme, with several assuming Beer-Lambert (BL) light attenuation,  
118 while only one employed a Delta-Eddington (DE) scheme. The majority of the models simulated ice algae only in the bottom  
119 sea-ice layer, either as a static or dynamic system, while two models were multi-layer models, simulating ice algae along the  
120 entire ice column. In terms of ecosystem complexity, models varied from simple Redfield-based models (RFD) with a single  
121 limiting nutrient, one algal group, and a detritus compartment to more comprehensive quota models with several functional  
122 groups, including ice bacteria, ice fauna, and multi-nutrient limitations.

123 **2.2 The N-ICE2015 Dataset**

124 The refrozen lead time series monitored during the N-ICE2015 expedition (Granskog et al., 2018) was selected as a test case  
125 for the model intercomparison due to the high frequency of available physical and biogeochemical measurements (e.g. Kauko  
126 et al., 2017; Olsen et al., 2017). The N-ICE expedition was a field campaign conducted aboard the RV *Lance*, which was  
127 frozen into pack ice north of Svalbard, drifting between approximately 83° and 80°N in the southern Nansen Basin of the  
128 Arctic Ocean between January and June 2015. Among the four ice floes monitored during the study period, the refrozen lead  
129 data were derived from Floe 3, which was studied from mid-April to early June 2015 as it drifted southward from 81.8° N to  
130 80.5° N.

132

**Table 1:** Sea-ice biogeochemical models participating in the 1D intercomparison project. BGC stands for biogeochemistry. Please see the main text for the remaining nomenclature used in the table.

Model/ Properties	BFM-SI	BFM-SI-Clim	CICE 5.1	CSIB-1D	SIESTA	SIMBA
<b>Ice Physics</b>	Modified SM 0L	Modified SM 0L	EC ML	SM 0L	EC ML	Prescribed
<b>Transport</b>	Growth/melt	Growth/melt	Growth/melt, brine drainage/diffus ion	Melt	Desalination	Growth/melt
<b>Radiation</b>	1 band; BL	1 band; BL	1 band; BL	1 band; BL	32 bands; DE	1 band; BL
<b>Grid for sea ice BGC</b>	1L, bottom, dynamic	1L, bottom, dynamic	Multi-layer	1L bottom static	Multi-layer	1L bottom static
<b>Sea-ice functional groups</b>	4N-2P-2D-1B-1Z	1N-1P-2D	3N-1P-1D	3N-1P-1D	4N-1P-1D	1N-1P-1D
<b>Cell quotas/Chl:C</b>	Quota/Prognostic	Quota/Prognostic	RFD/Constant	RFD/Constant	RFD/Constant	RFD/Constant
<b>Limiting element(s)</b>	Nitrogen, Phosphorous, Silicon	Silicon	Nitrogen, Silicon	Nitrogen, Silicon	Nitrogen, Phosphorous, Silicon	Nitrogen
<b>Ocean BGC</b>	1D slab	1D slab	n.a.	1D	n.a.	n.a.
<b>Area of model original tuning</b>	Greenland fjord (Arctic)	Greenland fjord (Arctic)	Barents Sea (Arctic)	Resolute Passage (Arctic)	Weddel Sea (Antarctic)	Central Arctic Ocean (Arctic)
<b>Reference</b>	Tedesco et al (2010)	Tedesco and Vichi (2014)	Duarte et al (2017)	Mortenson et al (2017)	Saenz and Arrigo (2014)	Castellani et al (2017)

134

135 The lead, approximately 400 m wide, opened on 23 April, began refreezing on 26 April, and was fully refrozen by 1 May. The  
 136 newly formed young ice in the lead was sampled from 6 May along a 100 m-long transect extending from the edge of the lead  
 137 toward its centre every 2–3 days until it broke up on 4 June (Kauko et al., 2017). The algal growth period occurred in April  
 138 and May. While the ice algal community was initially highly mixed, pennate diatoms of the genus *Nitzschia* became dominant  
 139 later in the season.

140

141 The N-ICE2015 refrozen lead time series was chosen for this intercomparison based on two key factors:

142

143 • Observational data availability: It provides sufficient observations (Kauko et al., 2017) for comparison with model  
144 simulations of physico-biogeochemical variables.

145 • Ancillary data availability: It includes detailed time series of atmosphere and ocean data, necessary to force model  
146 runs, and has been tested for feasibility in a previous 1D modelling study (Duarte et al., 2017).

147

148 **2.3 Experimental setup**

149 A strict protocol was developed and followed by all modelling groups. To accommodate the diversity of models, a minimum  
150 set of variables was selected for comparison with observations. These included sea-ice season timing, ice thickness, and snow  
151 thickness for coupled physical-biogeochemical models, as well as sea-ice nutrient concentrations and algal biomass  
152 (represented by Chl-a) for all models.

153

154 Two distinct experiments were conducted to assess model performance. The first experiment, labelled *no tuning*, aimed to run  
155 each model in its default configuration. The primary objective was to analyse the differences between model outputs and  
156 observational data and quantify the extent of biases. The intercomparison within this experiment sought to identify potential  
157 reasons for deviations from observations, such as the omission of key processes or inadequate parameterisations. The second  
158 experiment, labelled *tuning*, involved adjusting the models to better align with observed physical and biogeochemical  
159 properties. This experiment aimed to identify which processes needed to be modified or added, as well as the specific  
160 parameterisations or parameters that were adjusted and fine-tuned to improve agreement with observations.

161

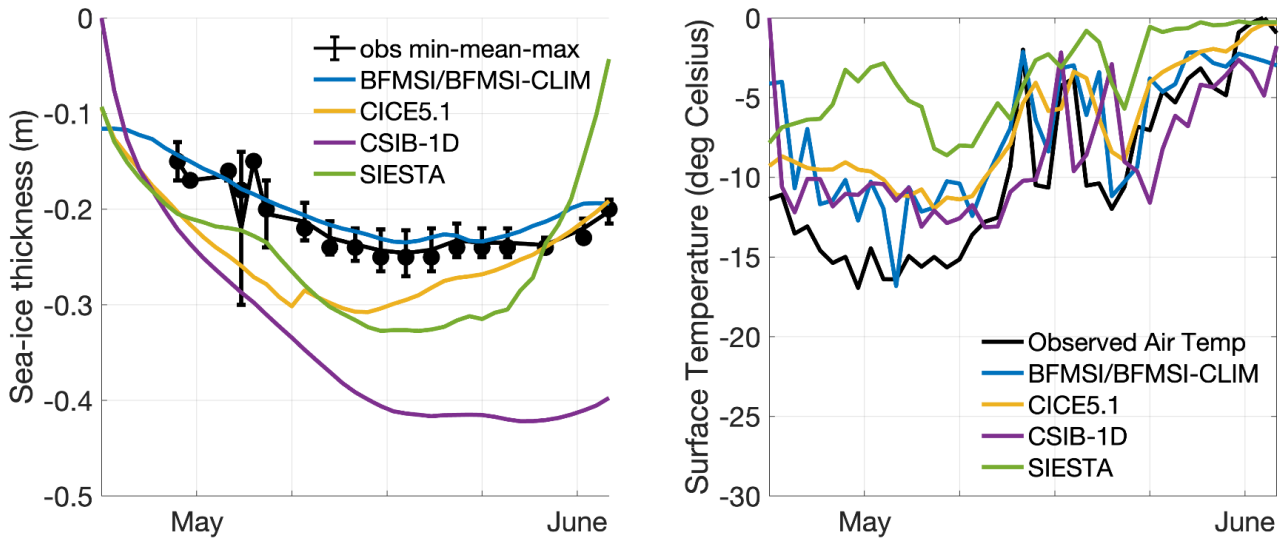
162 Both experiments were carried out independently by each modelling group, without prior knowledge of the work undertaken  
163 by others. This approach was adopted to eliminate potential biases, whether conscious or unconscious, during the  
164 implementation phase. To ensure a standardized comparison across models, all simulations used the same atmospheric and  
165 ocean forcing, as well as identical initial and boundary conditions, described in Duarte et al. (2017). Forcing time series  
166 included air temperature, precipitation, specific humidity, and wind speed (Hudson et al., 2015; Cohen et al., 2017); incident  
167 surface short and longwave radiation (Taskjelle et al., 2016; Hudson et al., 2016); sea ice temperature and salinity (Gerland et  
168 al., 2017); surface current velocity, heat fluxes, salinity, and temperature (Peterson et al., 2016, 2017); and ocean surface  
169 nutrient concentrations (Assmy et al., 2016). Atmospheric forcing was provided at hourly resolution, while oceanic forcing  
170 was available daily. For the sea-ice biogeochemical model without a thermodynamic component (i.e., SIMBA), observed ice  
171 and snow thickness data were provided. This standardised approach improved the comparability of the models, allowing for a  
172 robust evaluation of model performance. In the final phase, results were presented by each modelling group, and teams  
173 collaboratively discussed challenges, adjustments, and tuning choices.

174 **3. Results and discussion**

175 To support the interpretation of the biogeochemical models' performances, we first compared modelled and observed sea-ice  
 176 physical properties, in particular sea-ice thickness and surface (snow/ice) temperature (Fig. 1). While the models were forced  
 177 with 2 m air temperature, the surface temperature shown here refers to the simulated snow or ice surface temperature, which  
 178 may diverge from the atmospheric forcing depending on the model physics and surface energy budget. We did not include  
 179 snow thickness in this comparison, as observed values were relatively low and little variable, ranging between 2 and 6 cm  
 180 between 7 May and 3 June (Kauko et al., 2017) and thus had a limited influence on model differences for this specific case.

181

182 Observed sea-ice thickness shows relatively stable values around 0.2 m from early May to early June, with minor variability  
 183 in the observations (Fig. 1). Models with thermodynamic components (BFMSI/BFMSI-CLIM, CICE5.1, CSIB-1D, and  
 184 SIESTA) generally captured the observed thickness range and seasonal trend, although some diverge more notably. Surface  
 185 temperature simulations show stronger deviations across models. Although all models follow the overall seasonal warming  
 186 trend observed in the N-ICE2015 air temperature data (Fig. 1, right panel), the amplitude and short-term variability differ.  
 187 While some models reproduce much of the daily variability, others exhibit smoother or warmer biases. These differences in  
 188 physical conditions influenced light penetration and melt timing, which in turn affected the timing and magnitude of simulated  
 189 algal blooms, which will be analysed next.



190

191 **Figure 1:** Model results for sea-ice thickness (left) and surface temperature (right). Observations of sea-ice thickness are shown as dots for  
 192 the mean among replicates (at least 5 each) from different ice cores, while associated bars indicate the variability of the measurements  
 193 between their maximum and minimum. The observed air temperature is part of the forcings provided to the modelling groups (Hudson et  
 194 al., 2015; Cohen et al., 2017) and it is shown for comparison with modelled surface temperature.

195 Although the N-ICE refrozen lead resembles a typical ice season, in the *no tuning* experiment, none of the models accurately  
196 captured the observed algal phenology and bloom magnitude (Fig. 2, top left). All but one model underestimated Chl-a and  
197 produced a delayed bloom onset, though performances varied across diagnostic measures. Since most of the models tended to  
198 overestimate sea-ice thickness (Fig. 1), the delay in the simulated algal bloom could be attributed to reduced light transmittance  
199 through thicker ice. However, the delay also occurred in models that did not overestimate ice thickness, suggesting that other  
200 factors must have contributed to this bias. Due to limited nutrient data, few considerations can be drawn about simulated nutrient  
201 dynamics beyond an assessment of the potential model error's order of magnitude. Here, all but one model underestimated  
202 nitrate and silicate concentrations (Fig. 2, mid and bottom left), though all remained within a reasonable range.

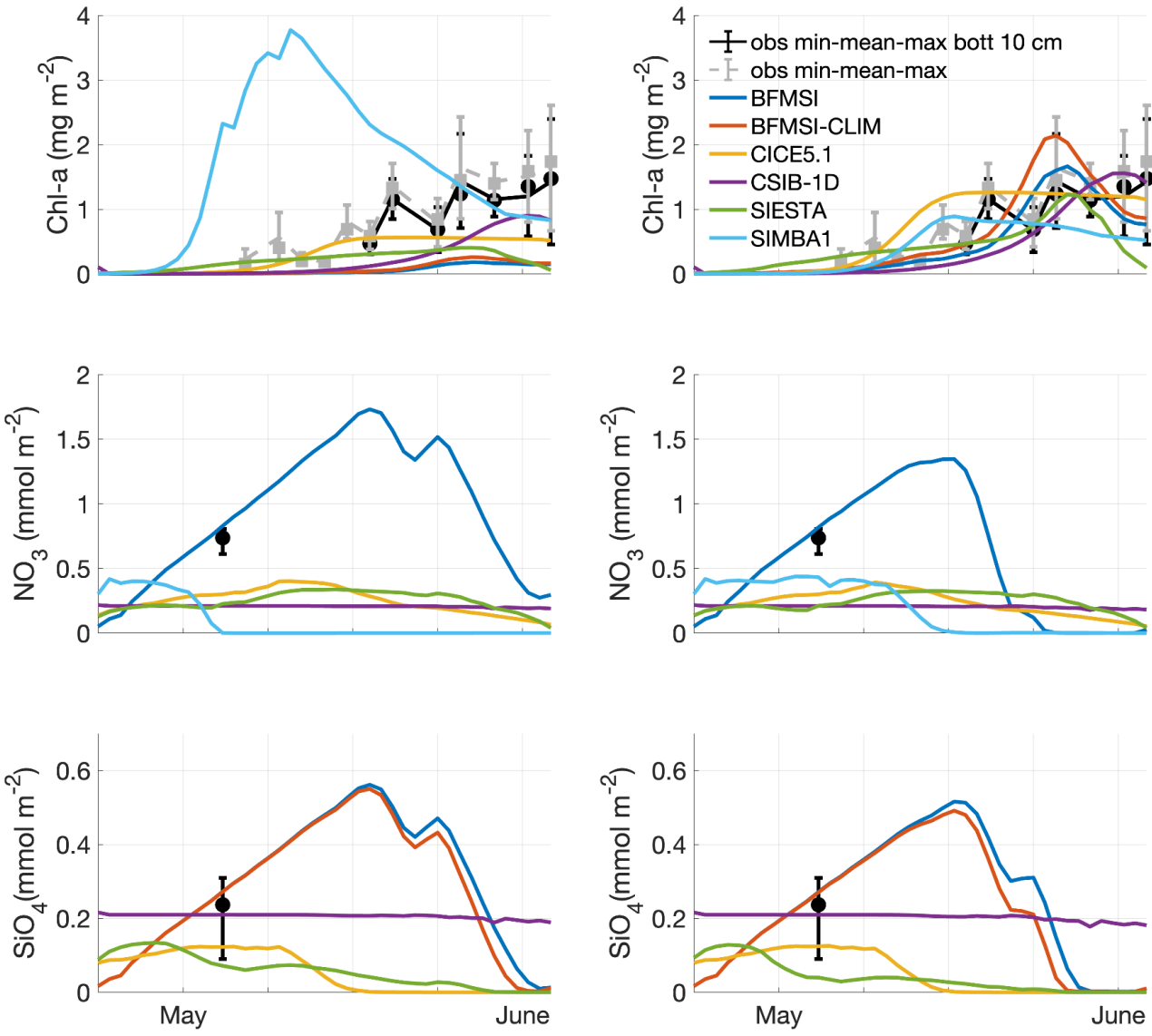
203  
204 In the *tuning* experiment, all models were able to reasonably simulate the ice algal phenology, though performance still varied  
205 across models (Fig. 2, top right). However, little improvement was achieved in the simulation of nitrate and silicate dynamics.  
206 Interestingly, tuning focused on different processes and parameters among models (Table 2), including:

207

- 208 • Change in the algal growth rate and/or in the size of the initial seeding population (initial ice algal biomass)
- 209 • The possibility of downward vertical migration of algae during melting
- 210 • Magnitude of silicic acid limitation by changing the half saturation constant and/or the nitrogen: silicon ratio of ice  
211 algae and/or the reference quota of silicon in sea-ice algae.

212  
213 Overall, all tuning strategies aimed to either lessen nutrient limitation or increase algal seeding or growth. However, despite  
214 tuning efforts, none of the models significantly improved the simulation of nitrate magnitude, except for BFM-SI, which was  
215 also the only model that did not underestimate nitrate and silicate before tuning (Fig. 2, mid and bottom left). When comparing  
216 nutrient parameterisations across models (Table 1), BFM-SI stands out as the only model in which the variability of the  
217 dynamic sea-ice BAL modulates the upward fluxes of dissolved inorganic matter. CSIB-1D also performed well in simulating  
218 the silicate dynamics, matching the magnitude of the observations before and after tuning. For most models, silicon had the  
219 strongest effect on ice algal growth during tuning, suggesting a potentially dominant role of silicon limitation. This would also  
220 explain why SIMBA was the only model that did not underestimate, but rather overestimated, ice algal growth, since it did not  
221 include silicon among its limiting nutrients.

222  
223 In general, models performed more poorly when simulating sea-ice nutrient dynamics. The limited improvement in nutrient  
224 representation compared to biomass can be attributed to model groups prioritising fitting simulations to Chl-a observations  
225 during the tuning phase, as these data were more temporally resolved and directly linked to the main focus of the study, i.e.,  
226 the ice algal bloom. In contrast, nutrient observations were limited to a single time point, which made them more difficult to  
227 constrain reliably. Nevertheless, despite the scarcity of available data, the simulation of nutrient processes appears poorly  
228 constrained, pointing to the need for more in-depth observational and experimental work.



229

230 **Figure 2:** Experiment with *no tuning* (left) and *tuning* (right). Model results for ice algae Chl-a (top),  
 231 nitrate (middle), and silicate (bottom).  
 232 Observations are shown as dots for the mean of the entire ice core or the bottom 10 cm (5 replicates each), while associated bars indicate the  
 233 variability of the measurements between their maximum and minimum measures.

234 The *tuning* experiment highlights the diversity of tuning parameters across models (Table 2), prompting critical questions  
 235 about model functionality and calibration. While models can be adjusted to align with observations, there is a risk of achieving

235 accurate results for the wrong reasons, particularly when tuning compensates for a missing or misrepresented process. In our  
236 case, none of our models included young ice formation. Observations indicate that a consistent fraction of the sea-ice sampled  
237 from the refrozen lead was granular (Graham et al., 2019), formed as frazil ice in turbulent conditions. As turbulence subsides,  
238 frazil crystals rise and can entrain suspended particles, including biological material, during acent, effectively concentrating  
239 them in the newly forming ice (Weeks and Ackley, 1982, Janssen et al., 2018). This may explain some of the tuning strategies,  
240 such as increases in algal growth rate (CSIB-1D) or the size of the initial seeding population (BFM-SI, BFM-SI-Clim).

241  
242 However, other factors likely influenced tuning choices as well. For example, some models used diatom Si:N ratios more  
243 appropriate for Antarctic waters, which overestimate the silica demand of Arctic diatoms. For example, CICE used a Si:N ratio  
244 close to 4:1, whereas Arctic diatoms may be closer to 1:1 (Duarte et al., 2017). In addition, the presence of relatively low Si:N  
245 ratios in Atlantic Water entering the region, as discussed in studies such as Duarte et al. (2021), supports the potential for silica  
246 limitation to emerge before nitrogen is exhausted. These regional nutrient characteristics and model structural features may  
247 have prompted tuning strategies involving relaxed silica limitation (BFM-SI, BFM-SI-Clim, CICE 5.1, and SIESTA).  
248 Furthermore, the apparent need to reduce nutrient limitation in order to simulate realistic biomass may indicate that ocean-to-  
249 ice nutrient fluxes are underestimated in some models (Duarte et al., 2022).

250  
251 Taken together, this intercomparison underscores how model tuning decisions can reveal not only numerical sensitivities but  
252 also areas where physical and biogeochemical process representations remain uncertain or incomplete. These insights are  
253 valuable for guiding future model development and targeted observations.

254

#### 255 **4. Conclusions**

256 This study presents an intercomparison of one-dimensional sea-ice biogeochemical models, evaluating their ability to simulate  
257 algal phenology, bloom magnitude, and nutrient dynamics in a refrozen lead environment. The results highlight significant  
258 disparities in model performance, with most models struggling to accurately reproduce the observed algal biomass and nutrient  
259 concentrations. For some models, this difficulty persisted even after tuning. While adjustments improved the representation of  
260 ice algal phenology, they had a limited impact on nutrient concentration across most models, emphasizing the challenges of  
261 parameterizing key processes such as nutrient fluxes and reinforcing the need for continued model development and validation  
262 supported by dedicated field and experimental observations.

263

264

265

266

267 **Table 2.** Comparison among models' performances before and after tuning. For reference, observed chlorophyll-a concentrations peaked  
 268 on 3 June at  $\sim 2.1 \text{ mg m}^{-3}$  in bottom sea ice and  $\sim 2.6 \text{ mg m}^{-3}$  in whole sea ice, aiding comparison of simulated bloom timing and magnitude.  
 269 Only parameters that were explicitly tuned are listed. Parameters not shown were kept at their default values or followed the standard initial  
 270 and boundary conditions provided for the intercomparison.

Model/ Properties	BFM-SI	BFM-SI-Clim	CICE 5.1	CSIB-1D	SIESTA	SIMBA
<b>Ice algal phenology before tuning</b>	Good algal growth timing but lower algal biomass.  Max [Chl-a] = 0.18 mg m <sup>-2</sup>  Day of the year of peak of Chl-a = 146	Good algal growth timing but lower algal biomass.  Max [Chl-a] = 0.26 mg m <sup>-2</sup>  Day of the year of peak of Chl-a = 146	Good algal growth timing but lower algal biomass.  Max [Chl-a] = 0.56 mg m <sup>-2</sup>  Day of the year of peak of Chl-a = 142	Good algal growth and lower algal biomass.  Max [Chl-a] = 0.90 mg m <sup>-2</sup>  Day of the year of peak of Chl-a = 152	Good algal growth timing but lower algal biomass.  Max [Chl-a] = 0.41 mg m <sup>-2</sup>  Day of the year of peak of Chl-a = 147	Earlier algal growth and higher algal biomass  Max [Chl-a] = 3.77 mg m <sup>-2</sup>  Day of the year of peak of Chl-a = 131
<b>Tuning strategy</b>	Lower silica limitation and higher algal biomass in seawater	Lower silica limitation and higher algal biomass in seawater	Lower silica limitation and reduced recruitment	Higher algal max spec growth rate	Active algal migration against brine movement and lower Si half-saturation constant.	Lower algal growth rate and removal of winter drainage of nutrients
<b>Parameter(s) before tuning</b>	Initial seawater [Chl-a] = 0.05 mg m <sup>-3</sup>  Reference Si quotum for adapted diatoms = 0.0085 mmol m <sup>-3</sup>	Initial seawater [Chl-a] = 0.05 mg m <sup>-3</sup>  Reference Si quotum for adapted diatoms = 0.0085 mmol m <sup>-3</sup>	Diatom Si:N ratio = 1.8 Half saturation for silicon uptake = 4.0 $\mu\text{M}$ Diatom boundary concentration = 0.002 $\mu\text{M}$	Chl-a max spec growth rate = 0.85 d <sup>-1</sup>	Algae fixed in ice layer grid; Half saturation of silicon uptake = 4.0 $\mu\text{M}$	Chl-a max spec growth rate = 0.86 d <sup>-1</sup>
<b>Parameter(s) after tuning</b>	Initial seawater [Chl-a] in = 0.5 mg m <sup>-3</sup>  Reference Si quotum for adapted diatoms = 0.0025 mmol m <sup>-3</sup>	Initial seawater [Chl-a] in = 0.5 mg m <sup>-3</sup>  Reference Si quotum for adapted diatoms = 0.0025 mmol m <sup>-3</sup>	Diatom Si:N ratio = 1.0 Half saturation for silicon uptake = 2.2 $\mu\text{M}$ Diatom boundary concentration = 0.0011 $\mu\text{M}$	Chl-a max spec growth rate increased to 0.95 d <sup>-1</sup>	Algae allowed to migrate downward with ice growth, up to 1.5 cm d <sup>-1</sup> ; Half saturation of silicon uptake = 1.0 $\mu\text{M}$	Chl-a max spec growth rate = 0.5 d <sup>-1</sup>

<b>Ice algal phenology after tuning</b>	Algal phenology and magnitude within observed range; Nitrate and silicate within range.  Max [Chl-a] = 1.67 mg m <sup>-2</sup>  Day of the year of peak of Chl-a = 146	Algal phenology and magnitude within observed range, Silicate within range.  Max [Chl-a] = 2.14 mg m <sup>-2</sup>  Day of the year of peak of Chl-a = 147	Algal phenology and magnitude within observed range; Lower nitrate, Silicate within range.  Max [Chl-a] = 1.26 mg m <sup>-2</sup>  Day of the year of peak of Chl-a = 141	Algal phenology and magnitude within observed range; Lower nitrate; Silicate within range.  Max [Chl-a] = 1.56 mg m <sup>-2</sup>  Day of the year of peak of Chl-a = 152	Algal phenology and magnitude within observed range; Earlier algal decay; Lower silicate and nitrate.  Max [Chl-a] = 1.23 mg m <sup>-2</sup>  Day of the year of peak of Chl-a = 147	Algal phenology and magnitude within observed range; Lower nitrate.  Max [Chl-a] = 0.89 mg m <sup>-2</sup>  Day of the year of peak of Chl-a = 137
---	--	--	---	---	--	--

271

272 The intercomparison highlights the unexpected challenges encountered in simulating a refrozen lead, primarily attributed to  
 273 the short ice season and the difficulty most models faced in accumulating sufficient sympagic (i.e., in-ice) biomass. In a future  
 274 Arctic Ocean characterized by increased lead openings, refreezing events, and young ice formation, there is an urgent need for  
 275 models to be able to represent such a dynamic environment. This study underscores the importance of understanding and  
 276 addressing the complexities involved in simulating specific and dynamic environmental scenarios.

277

278 The diversity of adjustments across models highlights both the range of tuning options available and the persisting knowledge  
 279 gaps. The insights gained contribute valuable knowledge to ongoing efforts aimed at refining and improving numerical models,  
 280 ensuring their accuracy and reliability in capturing complex interactions. To further advance this field of science, collaborative  
 281 and harmonized modelling developments are recommended. Variability in tuning strategies underscores key knowledge gaps  
 282 and the need for further model development using more coordinated approaches, such as common evaluation criteria and/or  
 283 shared parameter ranges. In doing so, sea-ice biogeochemical modelling can build on lessons learned from open-ocean  
 284 biogeochemical intercomparison and tuning efforts (e.g., Schartau et al., 2017), while addressing the unique challenges of  
 285 simulating sympagic systems. A *Phase 2* of the intercomparison would be highly valuable, potentially extending the study to  
 286 the variability of habitats that characterizes Antarctic sea ice. Collaborative sensitivity tests could be conducted, with all models  
 287 evaluating biological responses to the same tuning adjustments, tuning options could be expanded, and standard parameter  
 288 ranges could be revisited based on newer data collected in recent years. Increased clarity of model sensitivities would improve  
 289 future model robustness and enhance confidence in simulations of biogeochemical processes in ice-covered oceans.

290 **Code and data availability**

291 All relevant data, model code and numerical simulations presented in this work will be publicly made available upon  
 292 manuscript's acceptance.

293 **Author contributions**

294 LT and MV conceived the study. LT, GC, PD, EM, and BS produced the model runs. LT merged results from different models  
295 and wrote the first draft of the ms. All authors contributed to the analysis of results, discussion, and/or editing of the manuscript.

296 **Competing interests**

297 The authors declare no competing interests.

298 **Acknowledgements**

299 This work was written under the auspices of BEPSII (Biogeochemical Exchange Processes at the Sea-Ice Interfaces) Expert  
300 Group ([www.bepsii.org](http://www.bepsii.org)).

301 **Financial support**

302 LT and PD received funding from the European Union's Horizon 2020 research and innovation programme under grant  
303 agreement No 101003826 via project CRiceS (Climate relevant interactions and feedbacks: the key role of sea ice and snow  
304 in the polar and global climate system). GC, PD, and SM received funding from the RCN BREATHE project (Bottom sea ice  
305 Respiration and nutrient Exchanges Assessed for THE Arctic, #325405). PD and SM also received funding from the iC3 Center  
306 of Excellence (Centre for ice, Cryosphere, Carbon and Climate, #332635). EM received funding through ArcticNet and the  
307 National Science and Engineering Council in Canada. NS acknowledges Fisheries and Oceans Canada. Two in-person  
308 workshops were organized by the BEPSII Expert Group (Biogeochemical Exchange Processes at Sea Ice Interfaces) to support  
309 this work. These workshops were financially supported by the Scientific Committee on Antarctic Research (SCAR) and the  
310 World Climate Research Programme (WCRP) Climate and Cryosphere (CliC) core project.

311

312

313

314

315 **Appendix A**

316

317 **A1 Models description**

318

319 ***BFM-SI and BFM-SI-Clim***

320 *Overview*

321 The Biogeochemical Flux Model for sea ice (BFM-SI, Tedesco et al., 2010) is derived from the Biogeochemical Flux Model  
322 (BFM) framework (Vichi et al., 2023 and references therein), retaining its structure based on Chemical Functional Families  
323 (CFFs) and Living Functional Groups (LFGs). CFFs represent the elemental composition of living and non-living matter (C,  
324 N, P, Si, etc.), while LFGs describe groups of organisms with similar functional behaviour.

325 The model simulates biogeochemical processes within the Biologically Active Layer (BAL, Tedesco et al., 2010), the time-  
326 varying, permeable fraction of sea ice where liquid brine channels remain interconnected and biological activity can occur.  
327 This dynamic layer, typically located at the ice bottom, evolves according to physical conditions (e.g., temperature, salinity,  
328 brine volume) computed by a sea-ice physical model. The biological model simulates algal growth and elemental cycling only  
329 within this layer, assuming all biomass is confined to the permeable ice fraction continuously connected to seawater,  
330 maintaining full mass conservation at the ice–ocean–atmosphere interfaces.

331 The sea-ice physical model used in this study is ESIM (Enhanced Sea Ice Model). ESIM is a sea-ice thermodynamic model  
332 originally based on the Semtner 0-layer model (Semtner, 1976), but with more physical processes. It was initially built as a 1-  
333 D thermodynamic model of the sea-ice growth and decay (Tedesco et al., 2009), calculating vertical heat fluxes based on the  
334 1-dimensional heat conduction equation. ESIM has been later enhanced with a halodynamic component (Tedesco et al., 2010).  
335 Initial salt entrapment, gravity drainage, and flushing processes have been added to simulate the salinity evolution of the sea  
336 ice. In addition, the model takes into account other processes such as different forms of snow metamorphism (snow  
337 compaction, snow ice and superimposed ice formation). ESIM has been developed targeting biological applications, thus with

338 a focus on the physical requirements to model the biogeochemistry of the sea ice. The feature that makes this coupling possible  
339 is the innovative concept of the sea-ice BAL (Tedesco et al., 2010). The application of the BAL concept is more realistic than  
340 a prescribed static bottom BAL and is lighter than multi-layer models, thus it is suitable for large-scale applications without  
341 losing performance (Tedesco and Vichi, 2010, 2014).

342 *State variables and structure*

343 BFM-SI resolves 28 state variables organized as:

- 344     • 2 LFGs for sea-ice algae:
  - 345         1. Adapted diatoms (20–200  $\mu\text{m}$ ; Si-limited, highly acclimated)
  - 346         2. Surviving nanoflagellates (2–20  $\mu\text{m}$ ; low acclimation capacity)
- 347     • 1 LFG for sea-ice fauna
- 348     • 1 LFG for sea-ice bacteria
- 349     • 6 inorganic CFFs: phosphate, nitrate, ammonium, silicate, oxygen, carbon dioxide.
- 350     • 2 organic non-living CFFs: dissolved and particulate detritus.

351 Each algal group is described by up to five state variables (C, N, P, Si, and Chl), while ice fauna and bacteria up to three state  
352 variables (C, N, P). The model includes four macronutrients (phosphate, nitrate, ammonium, silicate), oxygen, and two detrital  
353 pools (dissolved and particulate, featuring up to 4 state variables C, N, P, Si). Biological processes include primary production  
354 respiration, exudation, nutrient uptake, lysis, and chlorophyll synthesis, with flexible stoichiometry (C:N:P:Si:Chl).

355 BFM-SI-Clim (Tedesco et al., 2014) is a simplified version of BFM-SI, retaining the same ecological dynamics, but including  
356 a reduced number of state variables. BFM-SI-Clim features only one single limiting macronutrient (Si) and one single group  
357 of sea ice algae (i.e. ice diatoms), same detritus and gases for totally 11 state variables.

358 *Coupling and boundary fluxes*

359 BFM-SI and BFM-SI-Clim are coupled online to the pelagic BFM with matching LFGs and CFFs.

- 360     • Ice–ocean fluxes: The entrainment or release of dissolved and particulate matter is proportional to ice growth/melt  
361         rate and brine volume.
- 362     • Ice–atmosphere fluxes: The nutrient input from snow and precipitation can be considered and scaled to snow-melt  
363         rate.

364 These exchanges ensure conservation of mass and consistent carbon, nutrient, and gas cycling across the interfaces.

365 *Applications and relevance*

366 BFM-SI represents the first process-based, biomass-explicit sea-ice biogeochemical model within a generalized marine  
367 biogeochemical framework. It can be used as a standalone 1-D module (Tedesco et al., 2010; Tedesco et al., 2012; Tedesco  
368 et al., 2014) or in coupled online or offline configuration to 3-D ocean circulation models (Tedesco et al., 2017; Tedesco et  
369 al., 2019) to study seasonal productivity, biomass export, and the contribution of sea-ice biogeochemistry to the global  
370 carbon cycle.

371

372 **CICE 5.1**

373 *Overview*

374 A comprehensive description of the Los Alamos Sea Ice Model physics and biogeochemistry may be found in Hunke et al.  
375 (2015) and Jeffery et al. (2016). The implementation used in the present work is detailed in Duarte et al. (2017). Therefore, in  
376 the next paragraphs we provide only a brief description of the model based on the cited references. There are two main  
377 approaches to simulate biogeochemical processes with CICE: one based on bottom ice biogeochemistry and another based on  
378 vertically-resolved biogeochemistry, which was used in the present study. This configuration uses a biogrid of variable height  
379 which overlaps part of the physical grid, used to compute thermodynamic processes. The number of layers of both grids is the  
380 same but their vertical resolution differs. The vertical extent of the biogrid is defined by the brine height which represents the  
381 sea ice vertical extent with an active brine network.

382 *State variables and structure*

383 The number of biogeochemical state variables in CICE biogeochemistry depends on user-defined options. In the simulations  
384 presented herein, these included brine height, the concentrations of nitrate, ammonium, silicic acid and diatom nitrogen. Brine  
385 concentrations are used for internal calculations and bulk values stored in model output files. The brine is exchanged across  
386 the layers of the biogrid and across the ice-ocean interface. These exchanges include brine drainage, driven by hydrostatic  
387 instability, and diffusion, driven by concentration gradients. Other exchanges occur during freezing and melting. In the case  
388 of sea ice inundation or snow melt, exchanges occur also at the ice-snow or ice-atmosphere interface. The biogeochemical  
389 model uses nitrogen as its “currency”. The model computes nutrient and silicic acid (in the case of diatoms) uptake by ice  
390 algae, remineralization and nitrification. Ice algal growth and production may be light, temperature or nutrient limited (nitrogen  
391 and silica, in the case of diatoms), following the Liebig’s law of minimum. Some tracers may cling to the ice matrix, such as  
392 ice algae, resisting expulsion during desalination, unlike dissolved nutrients.

393 *Coupling and boundary fluxes*

394 The CICE model may be coupled with ocean models and atmospheric models. We used a standalone configuration with an  
395 ocean slab layer as the bottom boundary. Time series of current velocities, heat fluxes, salinity, temperature, and nutrient  
396 concentrations forced the model. The atmosphere boundary was implemented using time series of air temperature, humidity,  
397 short and long wave radiation, precipitation, and wind velocity.

398 *Applications and relevance*

399 The CICE model is a community-type model used in several Earth System Models. It is one of the few models resolving  
400 biogeochemistry vertically.

401

402 **CSIB-1D**

403 *Overview*

404 The Canadian Sea Ice Biogeochemistry 1-Dimensional (CSIB-1D) model simulates ice algae and changes to nutrients within  
405 the ice. It is designed to simulate a sympagic ecosystem and biogeochemical processes coupled to a pelagic ecosystem in the  
406 underlying water column in order to represent the Arctic marine environment. An in-depth description of the development and  
407 application of this model can be found in Mortenson et al. (2017).

408 *State variables and structure*

409 The CSIB-1D ecosystem is represented by one functional sea-ice algal group dependent on three nutrients (silicate, nitrate and  
410 ammonium) in the lower skeletal layer of the sea ice, set as a default in the bottom 3 centimetres of the ice. The sea ice algae  
411 are limited by nutrients, light, and ice melt. The model uses a subgrid-scale non-uniform snow depth distribution to represent  
412 gradual snow melt and formation of melt ponds impacting light transmissions and heat fluxes during melt periods (Abraham  
413 et al., 2015). CSIB-1D ice algae are meant to represent diatoms, prevalent in the Arctic sea ice environment.

414 The ocean biogeochemistry model is a ten-compartment (small and large phytoplankton, microzooplankton, mesozooplankton,  
415 small and large detritus, biogenic silica, nitrate, ammonium, and silicate) based on Steiner et al. (2006). The module was  
416 updated by including mesozooplankton as a prognostic.

417 *Coupling and boundary fluxes*

418 Exchange of nutrients between the skeletal layer and the water column is by molecular diffusion and parameterized based on  
419 currents at the ice-water interface. The model is coupled to a physical-biogeochemical ocean model based on the General  
420 Ocean Turbulence Model (GOTM). GOTM provides the physical quantities required for computation of biogeochemical

421 variables in the water column, such as horizontal velocity fields, turbulent transports, photosynthetically active radiation  
422 (PAR), and temperature. They contribute to pelagic diatoms and detritus following Lavoie et al. (2009): sloughed ice algae  
423 enter either the large phytoplankton pool in which they continue to grow or the large detritus pool in which they sink rapidly  
424 as aggregate products in the coupled ocean model.

425 *Application and Relevance*

426 CSIB has been applied to studies on the evolution of the ice-water exchange of dissolved inorganic carbon (Mortenson et al.,  
427 2018) and ice-water-air exchange of dimethyl sulfide (Hayashida et al., 2017) in the marine Arctic.

428

429 **SIESSTA**

430 *Overview*

431 The Sea-Ice Ecosystem State (SIESSTA) model is a thermodynamic vertically-layered sea ice and snow model coupled to an  
432 algal ecosystem model. The model and associated equations and parameterizations are described in Saenz and Arrigo (2012,  
433 2014). The model was developed to vertically resolve sea ice brine processes (and associated nutrient transfer), sea ice optics,  
434 shortwave radiation transfer, and the sea ice algal productivity that is controlled by those processes. The model uses a minimum  
435 layer thickness of 2 cm. When the snow or ice thicknesses become greater than is resolved by the maximum number of layers  
436 (snow: 26, ice: 42), model layers grow and shrink in an accordion-fashion to preserve 2 cm resolution at the surface and snow-  
437 ice boundaries.

438 *State variables and structure*

439 Sea ice algae in SIESSTA is represented by a single (diatom) class of algae with a fixed stoichiometry, with internal units of  
440 carbon (mg/m<sup>3</sup>). Algae may be present in any layer of sea ice. Besides algal carbon, the ecological state variables used by the  
441 SIESSTA model include temperature, salinity, density, particulate organic carbon (detritus that is remineralized to liberate  
442 macronutrients), and 4 macronutrients (ammonium, nitrate, phosphate, silica). The model dynamically calculates sea ice brine  
443 density and volume, and has parameterizations of snow metamorphosis, sea ice surface melt and ponding, snow-ice formation,  
444 brine pumping and drainage, and enhanced convection in the skeletal layer of growing sea ice. Sea ice algae are considered  
445 motile and can migrate downward at a limited rate, but do not migrate upward and are considered released to the water column  
446 during bottom ice melt.

447 *Coupling and boundary fluxes*

448 SIESTA simulations in this manuscript were forced by time series of surface atmospheric and surface ocean parameters.  
449 SIESTA is mass- and energy-conservative to the accuracy of its 1st-order implicit solver. Coupling at the surface boundary  
450 requires the following atmospheric parameters: air temperature, wind speed, air pressure, dew point temperature, cloud cover  
451 (or downward longwave radiation), downwelling shortwave radiation) total precipitation. Coupling at the lower boundary  
452 requires the following surface ocean parameters: temperature, salinity, and macronutrient concentrations (ammonium, nitrate,  
453 phosphate, silica). SIESTA calculates, and can return to coupled models, energy and mass fluxes from the snow/ice/brine.  
454 Boundary flux calculations in SIESTA are derived from CICE version 4 (Hunke and Lipscomb, 2008).

455 *Applications and relevance*

456 SIESTA has been used to help bound the contribution of sea ice algae to overall Southern Ocean primary production (Saenz  
457 and Arrigo, 2014). SIESTA is also coupled to a 1-dimensional vertical ocean model (KPP-Ecosystem-Ice [KEI]) for  
458 investigation of dynamic-thermodynamic sea-ice-ocean-ecosystem controls and interactions (Saenz et al. 2023).

459  
460 **SIMBA**

461 *Overview*

462 A comprehensive description of the Sea Ice Model for Bottom Algae (SIMBA) can be found in Castellani et al. (2017).  
463 Different from Castellani et al. (2017) where the process of growth/melt was responsible for only algal loss, in the present  
464 study it is applied to nutrients as well, and it is responsible for nutrient replenishment in the bottom of the ice.

465 *State variables and structure*

466 SIMBA resolves only 3 state variables:

467     • 1 for sea-ice algae:  
468     • 1 for nutrients (nitrate)  
469     • 1 for detritus

470 The simulated biological processes are primary production and nutrient uptake, whereas respiration, mortality, and  
471 remineralization are taken as constant. Equations are solved in mmol N m-3. Equations are solved in the bottom of the ice, the  
472 thickness of the ice bottom can be set according to the available observations. In the case of N-ICE we use 10 cm.

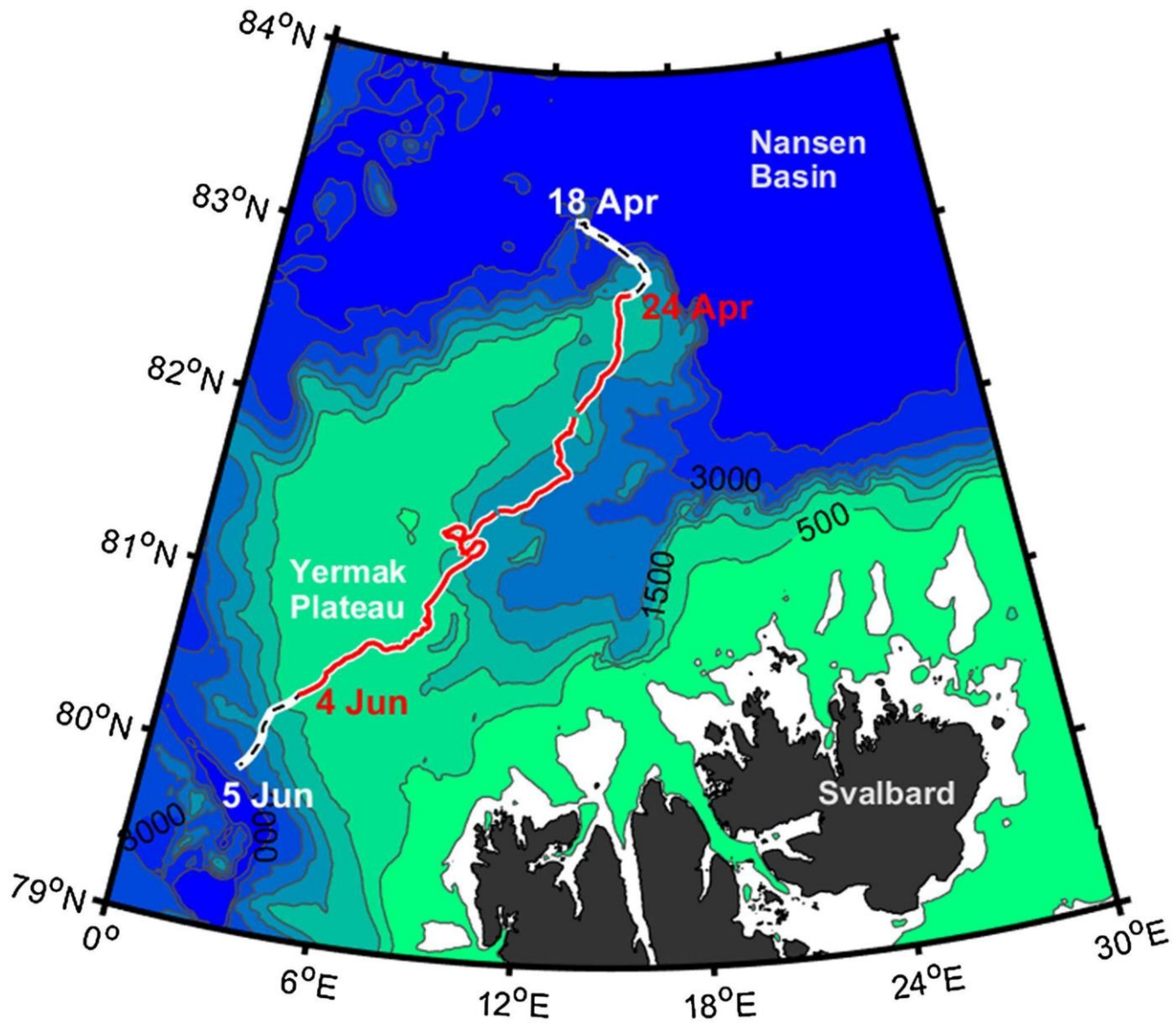
473 *Coupling and boundary fluxes*

474 SIMBA is coupled with the underlying ocean through the growth and melt processes which are responsible for nutrient  
475 exchanges and for algal loss. Ocean variables (i.e., nutrients concentrations, ocean currents, and ocean temperature) must be  
476 provided as forcing. Other required forcing includes ice and snow thickness, integrated downward shortwave radiation, and  
477 atmospheric temperature.

478 *Applications and relevance*

479 SIMBA was developed to study algal phenology on a pan-Arctic scale in two different environments: level ice and deformed  
480 ice. With this aim, SIMBA requires a prescribed physics. In Castellani et al. (2017) the physical constraints were provided by  
481 the MITgcm (Marshall et al., 1997; Losch et al, 2010). This characteristic of the model enhances its flexibility in applications  
482 and studies with different models (see e.g., Castellani et al., 2021).

483  
484



485  
486 **Figure A1.** RV Lance drift between 18 April and 5 June 2015 during the drift of Floe 3 of the N-ICE2015 expedition, from  
487 the Nansen Basin and across the Yermak Plateau. The segment corresponding to the time span of the simulations described in  
488 this study is shown in red (Duarte et al., 2017).  
489  
490  
491  
492  
493

494 **References**

495 Abraham, C., N. Steiner, A. Monahan, and C. Michel: Effects of subgrid-scale snow thickness variability on radiative transfer  
496 in sea ice, *J. Geophys. Res. Oceans*, 120, 5597–5614, doi:10.1002/2015JC010741, 2015.

497

498 Assmy, P., Duarte, P., Dujardin, J., Fernández-Méndez, M., Fransson, A., Hodgson, R., Kauko, H., Kristiansen, S., Mundy,  
499 C., Olsen, L. M., Peeken, I., Sandbu, M., Wallenschus, J., and Wold, A.: N-ICE2015 water column biogeochemistry [Dataset].  
500 Norwegian Polar Institute, doi: 10.21334/NPOLAR.2016.3EBB7F64, 2016.

501

502 Arrigo, K.R.: Sea ice as a habitat for primary producers, In D.N. Thomas (Ed.), *Sea Ice* (3rd ed., pp. 352–369). Wiley-  
503 Blackwell, doi:10.1002/9781118778371.ch14, 2017.

504

505 Boetius, A., Albrecht, S., Bakker, K., Bienhold, C., Felden, J., Fernández-Méndez, M., Hendricks, S., Katlein, C., Lalande, C.,  
506 Krumpen, T., Nicolaus, M., Peeken, I., Rabe, B., Rogacheva, A., Rybakova, E., Somavilla, R., and Wenzhöfer, F.: Export of  
507 algal biomass from the melting Arctic sea ice. *Science*, 339, 6126, 1430–1432, doi:10.1126/science.1231346, 2013.

508

509 Castellani, G., Losch, M., Lange, B. A., and Flores, H.: Modeling Arctic sea-ice algae: Physical drivers of spatial distribution  
510 and algae phenology, *J. Geophys. Res. Oceans*, 122, 7466–7487, doi:10.1002/2017JC012828, 2017.

511

512 Castellani, G., Tedesco, L., Steiner, N., Vancoppenolle, M.: Numerical model of sea-ice biogeochemistry, In D.N. Thomas  
513 (Ed.), *Sea Ice* (4th ed.). Wiley-Blackwell, In press doi:10.1002/9781394213764.ch20.

514

515 Castellani, G., Veyssiére, G., Karcher, M. et al. Shine a light: Under-ice light and its ecological implications in a changing  
516 Arctic Ocean, *Ambio* 51, 307–317, doi: 10.1007/s13280-021-01662-3, 2022.

517

518 Cohen, L., Hudson, S. R., Walden, V. P., Graham, R. M., and Granskog, M. A.: Meteorological conditions in a thinner Arctic  
519 sea ice regime from winter to summer during the Norwegian Young Sea Ice expedition (N-ICE2015), *J Geophys Res-Atmos*,  
520 122, 7235-7259, doi: 10.1002/2016JD026034, 2017.

521

522 Weeks, W. F., and Ackley, S. F. The growth, structure and properties of sea ice. *CRREL Monogr.* 82–1, 1982.

523

524 Dalman L. A., Meiners K. M., Thomas D. N., Deman F., Bestley S., Moreau S., Arrigo K. R., Campbell K., Corkill M., Cozzi  
525 S., Delille B., Fransson A., Fraser A. D., Henley S. F., Janssens J., Lannuzel D., Munro D. R., Nomura D., Norman L.,  
526 Papadimitriou S., Schallenberg C., Tison J.-L., Vancoppenolle M., van der Merwe P., Fripiat F.: Observation-based estimate

527 of net community production in Antarctic sea ice. *Geophysical Research Letters*, 52, e2024GL113717, doi:  
528 10.1029/2024GL113717, 2025.

529

530 Duarte, P., Assmy, P., Campbell, K., and Sundfjord, A.: The importance of turbulent ocean–sea ice nutrient exchanges for  
531 simulation of ice algal biomass and production with CICE6.1 and Icepack 1.2, *Geosci. Model Dev.*, 15, 841–857, doi:  
532 10.5194/gmd-15-841-2022, 2022.

533 Duarte, P., Meyer, A., & Moreau, S.: Nutrients in water masses in the Atlantic sector of the Arctic Ocean: Temporal trends,  
534 mixing and links with primary production, *Journal of Geophysical Research: Oceans*, 126, e2021JC017413, doi:  
535 10.1029/2021JC017413, 2021.

536

537 Duarte, P., Meyer, A., Olsen, L. M., Kauko, H. M., Assmy, P., Rosel, A., Itkin, P., Hudson, S. R., Granskog, M. A., Gerland,  
538 S., Sundfjord, A., Steen, H., Hop, H., Cohen, L., Peterson, A. K., Jeffery, N., Elliott, S. M., Hunke, E. C., and Turner, A. K.:  
539 Sea ice thermohaline dynamics and biogeochemistry in the Arctic Ocean: Empirical and model results, *J. Geophys. Res.-*  
540 *Biogeosci.*, 122, 1632–1654, doi: 10.1002/2016JG003660, 2017.

541

542 Eyring, V., Bony, S., Meehl, G. A., Senior, C. A., Stevens, B., Stouffer, R. J., and Taylor, K. E.: Overview of the Coupled  
543 Model Intercomparison Project Phase 6 (CMIP6) experimental design and organization, *Geosci. Model Dev.*, 9, 1937-1958,  
544 doi:10.5194/gmd-9-1937-2016, 2016.

545

546 Geoffroy, M., Bouchard, C., Flores, H., Robert, D., Gjøsæter, H., Hoover, C., Hop, H., Hussey, N. E., Nahrgang, J., Steiner,  
547 N., Bender, M., Berge, J., Castellani, G., Chernova, N., Copeman, L., David, C. L., Deary, A., Divoky, G., Dolgov, A. V.,  
548 Duffy-Anderson, J., Dupont, N., Durant, J. M., Elliott, K., Gauthier, S., Goldstein, E. D., Gradinger, R., Hedges, K., Herbig,  
549 J., Laurel, B., Loseto, L., Maes, S., Mark, F. C., Mosbech, A., Pedro, S., Pettitt-Wade, H., Prokopchuk, I., Renaud, P. E.,  
550 Schembri, S., Vestfals, C., Walkusz, W.; The circumpolar impacts of climate change and anthropogenic stressors on Arctic  
551 cod (*Boreogadus saida*) and its ecosystem. *Elementa: Science of the Anthropocene*, 11, 1: 00097. doi:  
552 10.1525/elementa.2022.00097, 2023.

553

554 Gerland, S., Granskog, M. A., King, J., and Rösel, A.: N-ICE2015 ICE core physics: Temperature, salinity and density [data  
555 set], Norwegian Polar Institute, doi: 10.21334/npolar.2017.c3db82e3, 2017.

556

557 Graham, R.M., Itkin, P., Meyer, A. et al.: Winter storms accelerate the demise of sea ice in the Atlantic sector of the Arctic  
558 Ocean. *Sci Rep* 9, 9222, doi: 10.1038/s41598-019-45574-5, 2019.

559

560 Granskog, M. A., Fer, I., Rinke, A., and Steen, H.: Atmosphere-Ice-Ocean-Ecosystem Processes in a Thinner Arctic Sea

561 Ice Regime: The Norwegian Young Sea ICE (N-ICE2015) Expedition, *J. Geophys. Res.-Oceans*, 123, 1586–1594,  
562 doi: 10.1002/2017jc013328, 2018.

563

564 Hayashida, H., Jin, M., Steiner, N. S., Swart, N. C., Watanabe, E., Fiedler, R., Hogg, A. McC., Kiss, A. E., Matear, R. J., and  
565 Strutton, P. G.: Ice Algae Model Intercomparison Project phase 2 (IAMIP2), *Geosci. Model Dev.*, 14, 6847–6861,  
566 <https://doi.org/10.5194/gmd-14-6847-2021>, 2021.

567

568 Hayashida, H., Steiner, N., Monahan, A., Galindo, V., Lizotte, M., and Levasseur, M.: Implications of sea-ice biogeochemistry  
569 for oceanic production and emissions of dimethyl sulfide in the Arctic, *Biogeosciences*, 14, 3129–3155, doi: 10.5194/bg-14-  
570 3129-2017, 2017.

571

572 Hudson, S. R., Cohen, L., and Walden, V. P.: N-ICE2015 surface meteorology [data set], Norwegian Polar Institute,  
573 <https://doi.org/10.21334/npolar.2015.056a61d1>, 2015.

574

575 Hudson, S. R., Cohen, L., and Walden, V. P.: N-ICE2015 surface broadband radiation data [data set]. Norwegian Polar  
576 Institute, <https://doi.org/10.21334/npolar.2016.a89cb766>, 2016.

577

578 Hunke, E. C., and W. H. Lipscomb: CICE: The Los Alamos Sea Ice Model: Documentation and software user's manual,  
579 version 4.0, Tech. Rep. LA-CC-06-012, Los Alamos Natl. Lab., Los Alamos, N. M., 2008.

580

581 Hunke, E. C., Lipscomb, W. H., Turner, A. K., Jeffery, N., and Elliot, S.: CICE: The Los Alamos sea ice model documentation  
582 and user's manual version 5.1. Tech. Rep., LA-CC-06-012, Los Alamos National Laboratory, Los Alamos, N. M, 2015.

583

584 Janssens, J., Meiners, K. M., Townsend, A. T., Lannuzel, D.: Organic matter controls of iron incorporation in growing sea ice,  
585 *Frontiers in Earth Science* 6: 22, doi: 10.3389/feart.2018.00022, 2018.

586

587 Jeffery, N., Elliott, S., Hunke, E. C. , Lipscomb, W. H. and Turner, A. K.: Biogeochemistry of CICE: The Los Alamos Sea Ice  
588 Model, Documentation and User's Manual. *Zbgc\_colpkg* modifications to Version 5, Los Alamos National Laboratory, Los  
589 Alamos, N. M., 2016.

590

591 Kauko, H. M., Taskjelle, T., Assmy, P., Pavlov, A. K., Mundy, C. J., Duarte, P., Fernández-Méndez, M., Olsen, L. M., Hudson,  
592 S. R., Johnsen, G., Elliot, A., Wang, F., Granskog, M. A.: Windows in Arctic sea ice: light transmission and ice algae in a  
593 refrozen lead, *J. Geophys. Res.-Biogeo.*, 122, doi:10.1002/2016JG003626, 2017.

594

595 Koch, C. W., Brown, T. A., Amiraux, R. et al. Year-round utilization of sea ice-associated carbon in Arctic ecosystems, Nat  
596 Commun 14, 1964, doi:10.1038/s41467-023-37612-8, 2023.

597

598 Kohlbach D., Lange B. A., Schaafsma, F. L., David, C., Vortkamp, M., Graeve, M., van Franeker, J. A., Krumpen, T., and  
599 Flores, H.: Ice Algae-Produced Carbon Is Critical for Overwintering of Antarctic Krill *Euphausia superba*, Front. Mar. Sci.  
600 4:310, doi:10.3389/fmars.2017.00310, 2017.

601

602 Lannuzel, D, Tedesco, L., van Leeuwe, M., Campbell, K., Flores, H., Delille, B., Miller, L., Stefels, J., Assmy, P., Bowman,  
603 J., Brown, K., Castellani, G., Chierici, M., Crabeck, O., Damm, E., Else, B., Fransson, A., Fripiat, F., Geilfus, N.-X., Jacques,  
604 C., Jones, E., Kaartokallio, K., Kotovitch, M., Meiners, K., Moreau, S., Nomura, D., Peeken, I., Rintala, J.-M., Steiner, N.,  
605 Tison, J.-L., Vancoppenolle, M., der Linden, F. V., Vichi, M., Wongpan, P.: The future of Arctic sea-ice biogeochemistry  
606 and ice-associated ecosystems, Nature Climate Change, doi:10.138/s41558-020-00940-4, 2020.

607

608 Losch, M., D. Menemenlis, J. M. Campin, P. Heimbach, and C. Hill: On the formulation of sea-ice models: Part 1: Effects of  
609 different solver implementations and parameterizations, Ocean Modell., 33, 129–144, doi:10.1016/j.ocemod.2009.12.008,  
610 2010.

611

612 Marshall, J., A. J. Adcroft, C. N. Hill, L. Perelman, and C. Heisey: A finite-volume, incompressible Navier Stokes model for  
613 studies of the ocean on parallel computers, J. Geophys. Res., 102(C3), 5753–5766, doi:10.1029/96JC02775, 1997.

614

615 Mortenson, E., Hayashida, H., Steiner, N., Monahan, A., Blais, M., Gale, M. A., Galindo, V., Gosselin, M., Hu, X., Lavoie,  
616 D., Mundy, C. J.: A model-based analysis of physical and biological controls on ice algal and pelagic primary production in  
617 Resolute Passage, Elementa: Science of the Anthropocene Sci Anth, 5, 39, doi:10.1525/elementa.229, 2017.

618

619 Mortenson, E., Steiner, N., Monahan, A. H., Miller, L. A., Geilfus, N.-X., & Brown, K., A model-based analysis of physical  
620 and biogeochemical controls on carbon exchange in the upper water column, sea ice, and atmosphere in a seasonally ice-  
621 covered Arctic strait. Journal of Geophysical Research: Oceans, 123, 7529–7549, doi: 10.1029/2018JC014376, 2018.

622

623 Olsen, L. M., Laney, S. R., Duarte, P., Kauko, H. M., Fernández-Méndez, M., Mundy, C. J., Rösel, A., Meyer, A., Itkin, P.,  
624 Cohen, L., Peeken, I., Tatarek, A., Rózańska, M., Wiktor, J., Taskjelle, T., Pavlov, A. K., Hudson, S. R., Granskog, M. A.,  
625 Hop, H., and Assmy, P.: The seeding of ice-algal blooms in Arctic pack ice: the multiyear ice seed repository hypothesis,  
626 Journal of Geophysical Research: Biogeosciences, 10.1002/2016jg003668, 2017.

627

628 Peterson, A. K., Fer, I., Randelhoff, A., Meyer, A., Håvik, L., Smedsrød, L. H., Onarheim, L., Muilwijk, M., Sundfjord, A.,  
629 and McPhee, M. H.: N-ICE2015 ocean turbulent fluxes from under-ICE turbulence cluster (TIC) [data set], Norwegian Polar  
630 Institute, <https://doi.org/10.21334/npolar.2016.ab29f1e2>, 2016.

631

632 Peterson, A. K., Fer, I., McPhee, M. G., and Randelhoff, A.: Turbulent heat and momentum fluxes in the upper ocean under  
633 Arctic sea ice, *Journal of Geophysical Research: Oceans*, 122, 1439–1456, doi:10.1002/2016JC012283, 2017.

634

635 Post, E., Bhatt, U. S., Bitz, C. M., Brodie, J. F., Fulton, T. L., Hebblewhite, M., Kerby, J., Kutz, S. J., Stirling, I., Walker D.  
636 A. et al.: Ecological consequences of sea-ice decline, *Science*, 341(6145), 519–524, doi:10.1126/science.1235225, 2013.

637

638 Poulin, M., Daubjerg, N., Gradinger, R., Ilyash, L. V., Ratkova, T. N., von Quillfeldt, C.: The pan-Arctic biodiversity of  
639 marine pelagic and sea-ice unicellular eukaryotes: a first-attempt assessment, *Mar. Biodiv.*, 41, 13–28, doi:10.1007/s12526-  
640 010-0058-8, 2011.

641

642 Saenz, B. T., and Arrigo, K. R.: Simulation of a sea ice ecosystem using a hybrid model for slush layer desalination, *J. Geophys.  
643 Res.*, 117, C05007, doi:10.1029/2011JC007544, 2012.

644

645 Saenz, B. T., and Arrigo, K. R.: Annual primary production in Antarctic sea ice during 2005–2006 from a sea ice state estimate,  
646 *J. Geophys. Res. Oceans*, 119, 3645–3678, doi:10.1002/2013JC009677, 2014.

647

648 Saenz, B. T., McKee, D. C., Doney, S. C., Martinson, D. G., Stammerjohn, S. E: Influence of seasonally varying sea-ice  
649 concentration and subsurface ocean heat on sea-ice thickness and sea-ice seasonality for a ‘warm-shelf’ region in Antarctica.  
650 *Journal of Glaciology*, 69(277):1466-1482, doi:10.1017/jog.2023.36, 2023.

651

652 Schaafsma, F. L., D. Kohlbach, C. David, B. A. Lange, M. Graeve, H. Flores, and J. A. van Franeker: Spatio-temporal  
653 variability in the winter diet of larval and juvenile Antarctic krill, *Euphausia superba*, in ice-covered waters, *Marine Ecology  
654 Progress Series*, 580, 101-115, doi: [doi.org/10.3354/meps12309](https://doi.org/10.3354/meps12309), 2017.

655

656 Semtner, A. J.: A model for the thermodynamic growth of sea ice in numerical investigation of climate, *J. Phys. Oceanogr.*,  
657 6:379–389, doi: 10.1175/1520-0485(1976)006<0379:AMFTTG>2.0.CO;2, 1976.

658

659 Schartau, M., Wallhead, P., Hemmings, J., Löptien, U., Kriest, I., Krishna, S., Ward, B. A., Slawig, T., and Oschlies, A.:  
660 Reviews and syntheses: parameter identification in marine planktonic ecosystem modelling, *Biogeosciences*, 14, 1647–1701,  
661 doi: 10.5194/bg-14-1647-2017, 2017.

662  
663 Steiner, N., Bowman, J., Campbell, K., Chierici, ...M., Eronen-Rasimus, Falardeau , E. M., Flores, H., Fransson , A., Herr ,  
664 H., Insley , S. J., Kauko, H., Lannuzel, D., Loseto, L., Lynnes , A., Majewski , A., Meiners , K., Miller, L.. A., Michel, L.,  
665 Moreau, S., Nacke , M., Nomura, D., Tedesco, L., van Franeker, J. A., van Leeuwe, M. A., Wongpan, P.: Climate change  
666 impacts on sea-ice ecosystems and associated ecosystem services, *Elem Sci Anth*, 9 (1): 00007,  
667 doi:10.1525/elementa.2021.00007, 2021.

668  
669 Taskjelle, T., Hudson, S. R. , Pavlov, A., and Granskog, M. A.: N-ICE2015 surface and under-ICE spectral shortwave radiation  
670 data [data set], Norwegian Polar Institute, <https://doi.org/10.21334/npolar.2016.9089792e>, 2016.

671  
672 Tedesco, L., Vichi, M., Haapala, J., Stipa, T.: An enhanced sea-ice thermodynamic model applied to  
673 the Baltic Sea. *Boreal Environmental Research* 14, 68–80.<http://www.borenv.net/BER/pdfs/ber14/ber14-068.pdf>, 2009.

674  
675 Tedesco, L., Miettunen E., An, B.W., Kaartokallio, H., Haapala, J.: Long-term mesoscale variability of modelled sea-ice  
676 primary production in the northern Baltic Sea. *Elem. Sci. Anth.*, 5: 29, doi: 10.1525/elementa.223, 2017.

677  
678 Tedesco, L., Vichi, M.: Sea ice biogeochemistry: a guide for modellers, *PLOS ONE*, doi:10.1371/journal.pone.0089217, 2014.

679  
680 Tedesco, L., Vichi, M., Haapala, J., and Stipa, T.: A dynamic Biologically-Active Layer for numerical studies of the sea ice  
681 ecosystem, *Ocean Modelling*, 35(1-2):89-104, doi:10.1016/j.ocemod.2010.06.008, 2010.

682  
683 Tedesco, L., Vichi, M., Scoccimarro, E.: Sea-ice algal phenology in a warmer Arctic, *Science Advances*,5, eaav4830, doi:  
684 10.1126/sciadv.aav4830, 2019.

685  
686 Tedesco, L., Vichi, M., Thomas, D.: Process studies on the ecological coupling between sea ice algae and phytoplankton,  
687 *Ecological Modelling*, 226: 120-138, doi:10.1016/j.ecolmodel.2011.11.011, 2012.

688  
689 Watanabe, E., Jin, M., Hayashida, H., Zhang, J., & Steiner, N.: Multi-Model Intercomparison of the Pan-Arctic Ice-Algal  
690 Productivity on Seasonal, Interannual, and Decadal Timescales, *Journal of Geophysical Research: Oceans*, 124, 9053–9084.  
691 doi:10.1029/2019JC015100, 2019.